Металлофиз. новейшие технол. / Metallofiz. Noveishie Tekhnol.
2017, т. 39, № 7, сс. 959–981 / DOI: 10.15407/mfint.39.07.0959
Оттиски доступны непосредственно от издателя
Фотокопирование разрешено только
в соответствии с лицензией

ФАЗОВЫЕ ПРЕВРАЩЕНИЯ

PACS numbers: 07.05.Tp, 61.72.Qq, 64.70.dg, 81.05.Bx, 81.20.Hy, 81.30.Fb

Shrinkage Estimation of Cast Al–Si Alloys Through Process Simulation

Samavedam Santhi and Srinivasan Sundarrajan*

Mahatma Gandhi Institute of Technology,
500075 Hyderabad, India
**National Institute of Technology,*
620015 Trichy, India

With the advent of various casting process simulation techniques, it is possible to derive theoretically casting parameters, which can be further validated through experiments. In this paper, detailed simulation activities are carried out to determine the shrinkage characteristics of two Al–Si alloys (US 413 and US A356) followed by validation through experimental studies. Production of defect-free castings requires good understanding of shrinkage characteristics. The influence of various process parameters on these characteristics determines the casting quality. Based on this, an extensive study is undertaken to comprehend the influence of various parameters.

Keywords: shrinkage, cast aluminium alloys, casting mould, process simulation, solid model, design of experiments.

З появою різних метод моделювання процесу лиття з'явилася можливість теоретично оцінити параметри лиття, які можуть бути додатково перевірені за допомогою експериментів. В даній роботі було проведено детальне моделювання для визначення характеристик усадки двох стопів Al–Si (US 413 і US A356) з подальшою перевіркою за допомогою експерименту. Виробництво виливків без дефектів потребує доброго розуміння характеристик усадки. Вплив різних параметрів процесу на ці характеристики визначає якість виливки. Виходячи з цього, було проведено цілу низку досліджень, щоб визначити вплив різних параметрів.

Ключові слова: усадка стопу, ливарні алюмінійові стопи, ливарна форма,

Corresponding author: Samavedam Santhi
E-mail: santhi_samave@yahoo.com

Please cite this article as: Samavedam Santhi and Srinivasan Sundarrajan, Shrinkage Estimation of Cast Al–Si Alloys through Process Simulation, *Metallofiz. Noveishie Tekhnol.*, **39**, No. 7: 959–981 (2017), DOI: 10.15407/mfint.39.07.0959.

симуляція процесу, модель твердого тіла, проєктування експериментів.

С появлением различных методов моделирования процесса литья появилась возможность теоретически оценить параметры литья, которые могут быть дополнительно проверены с помощью экспериментов. В данной работе было проведено детальное моделирование для определения характеристик усадки двух сплавов Al–Si (US 413 и US A356) с последующей проверкой с помощью эксперимента. Производство отливок без дефектов требует хорошего понимания характеристик усадки. Влияние различных параметров процесса на эти характеристики определяет качество отливки. Исходя из этого, было проведено обширное исследование, чтобы определить влияние различных параметров.

Ключевые слова: усадка сплава, литые алюминиевые сплавы, литейная форма, моделирование процессов, модель твёрдого тела, проектирование экспериментов.

(Received June 29, 2017)

1. INTRODUCTION

Solidification of castings involves modification of phase with liberation of latent heat from a moving liquid-solid boundary to mould and then to atmosphere [1]. Casting process simulation programmes are time and temperature dependent and more attention is being focused on systematic aspects in production of castings such as studies of the heat transfer mechanisms, by which castings solidify, and the rate, at which solidification and shrinkage takes place [2].

Computer simulation of casting takes into account the qualitative and quantitative consideration of the process parameters, boundary conditions and their influence on quality of casting. Process parameters and boundary conditions include casting type, mould material, chemical composition of alloy considered, physical properties and interfacial heat transfer coefficient between the existing boundaries.

The temperature history of all sites inside the casting are attained by plotting the progress of solidification fronts (isothermal contours) at different instants of time, and by identifying the last freezing regions/sites [3]. The numerical simulation of casting solidification procedure has been done through Finite Difference Method (FDM).

The cast Al–Si alloys are the true workhorses of the aluminium alloy casting industry because of their excellent casting characteristics and good strength [4]. Shrinkage is the most significant discontinuity in castings, and forms due to the contraction of liquid metal, transformation of liquid to the solid and contraction in the solid state [5]. This shrinkage results in the form of voids like micro- and macroshrinkage during solidification. Macroporosity or macroshrinkage occurs due to entrapped liquid metal surrounded by solid. Y. Li states [6] that the

tendency for formation of shrinkage porosity is related to liquid to solid volume fraction at the time of final solidification and solidification temperature range of alloy. Shape and relevant wall thickness of a casting are very important casting parameters that influence the shrinkage porosity.

2. SIMULATION PROCEDURE

Efficient design of experiments is an efficient approach for improving a process to quickly obtain meaningful results and draw conclusions about how factors or process parameters interact [7, 8] when more than one factor is changing at a time. An orthogonal array would mean a balanced design with equal weight age to each factor [9, 10]. MINITAB software was used for experimental design [10].

2.1. Selection of Process Parameters

The parameters, which influence the shrinkage, are pouring temperature, casting shape, use of chills, alloy composition, type of mould sand, presence of mould coat and pouring time [11].

Out of the above parameters, which influence the shrinkage, alloy composition, bottom chill, shape of the casting, mould coat, and pouring temperature, were considered as the process parameters for the present investigation. Alloy composition affects the shrinkage characteristics and mechanical properties of the cast product. To study the influence of alloy composition, two alloys with chemical compositions given in Table 1 (US 413 and US A356) were used.

TABLE 1. Chemical composition (wt.%).

Element	US 413	US A356
Silicon	11.5	6.90
Iron	0.40	0.45
Copper	0.15	0.20
Manganese	0.55	0.35
Magnesium	0.10	0.55
Nickel	0.10	0.15
Zinc	0.15	0.15
Lead	0.10	0.15
Tin	—	0.05
Titanium	0.20	0.15
Others (each)	0.05	0.05
Others (total)	0.15	0.15
Aluminium	Balance	Balance

TABLE 2. Dimensional details of the casting shapes to determine shrinkage characteristics.

Sl. No.	Shape	Dimension, mm	Pouring position	Surface area, cm^2	Volume, cm^3
1	Rectangle	115×100×48	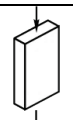	436.40	552.000
2	Cube	82×82×82		403.44	551.368
3	Cylinder	∅90×90		381.51	572.265

Rectangle, cube and cylinder were the three basic industrial casting shapes considered for the present study. The rate of heat exchange depends on thermo-physical properties of the liquid metal, casting mould, wall thickness of casting and its shape. The dimensional details of the casting are provided in Table 2.

Mould coatings provide smooth surfaces, improve the quality and reduce the mould erosion [1, 12]. Pouring temperature [13] influences fluidity, porosity, strength and structure of the casting. Pouring temperature T (T is melting point +75°C) and $T + 50$°C of superheat was considered. The bottom chill showed significant difference in the casting characteristics, and directional solidification can help in eliminating shrinkage porosity defects [14]. A mild steel (MS) chill was considered for the present study.

Table 3 shows the details of the factors and their levels (variables) for the present study. An orthogonal array $L36$ (2^4 3^1) was used with five factors (one process parameter with three levels and four process parameters with two levels) and 36 runs for shrinkage simulation investigation, as shown in Table 4.

TABLE 3. Factors and their levels for shrinkage simulation studies.

	Factor 1 Alloy	Factor 2 Chill	Factor 3 Pouring temperature, °C	Factor 4 Mould coat	Factor 5 Casting mould
Level 1	US A356	Mild Steel (MS)	$T + 50$	Graphite (GC)	Cylinder
Level 2	US 413	No	T	No coating (NC)	Cube
Level 3	—	—	—	—	Rectangle

TABLE 4. $L36$ ($2^4\,3^1$) orthogonal array for the simulation studies.

Simulation run order	Alloy	Chill	Pouring temperature, °C	Mould coat	Casting mould
1	US A356	MS	$T + 50$	GC	Cylinder
2	US A356	MS	$T + 50$	GC	Cube
3	US A356	MS	$T + 50$	GC	Rectangle
4	US A356	MS	$T + 50$	NC	Cylinder
5	US A356	MS	$T + 50$	NC	Cube
6	US A356	MS	$T + 50$	NC	Rectangle
7	US A356	MS	T	GC	Cylinder
8	US A356	MS	T	GC	Cube
9	US A356	MS	T	NC	Rectangle
10	US A356	No	$T + 50$	NC	Cylinder
11	US A356	No	$T + 50$	NC	Cube
12	US A356	No	$T + 50$	GC	Rectangle
13	US A356	No	T	GC	Cylinder
14	US A356	No	T	GC	Cube
15	US A356	No	T	GC	Rectangle
16	US A356	No	T	NC	Cylinder
17	US A356	No	T	NC	Cube
18	US A356	No	T	NC	Rectangle
19	US 413	MS	T	NC	Cylinder
20	US 413	MS	T	NC	Cube
21	US 413	MS	T	NC	Rectangle
22	US 413	MS	T	GC	Cylinder
23	US 413	MS	T	GC	Cube
24	US 413	MS	T	GC	Rectangle
25	US 413	MS	$T + 50$	NC	Cylinder
26	US 413	MS	$T + 50$	NC	Cube
27	US 413	MS	$T + 50$	NC	Rectangle
28	US 413	No	T	GC	Cylinder
29	US 413	No	T	GC	Cube
30	US 413	No	T	GC	Rectangle
31	US 413	No	$T + 50$	NC	Cylinder
32	US 413	No	$T + 50$	NC	Cube
33	US 413	No	$T + 50$	NC	Rectangle
34	US 413	No	$T + 50$	GC	Cylinder
35	US 413	No	$T + 50$	GC	Cube
36	US 413	No	$T + 50$	GC	Rectangle

3. CASTING PROCESS SIMULATION

3.1. Solid Model

Simulation studies on shrinkage characteristics of aluminium alloy have been conducted using the Virtual casting commercial software

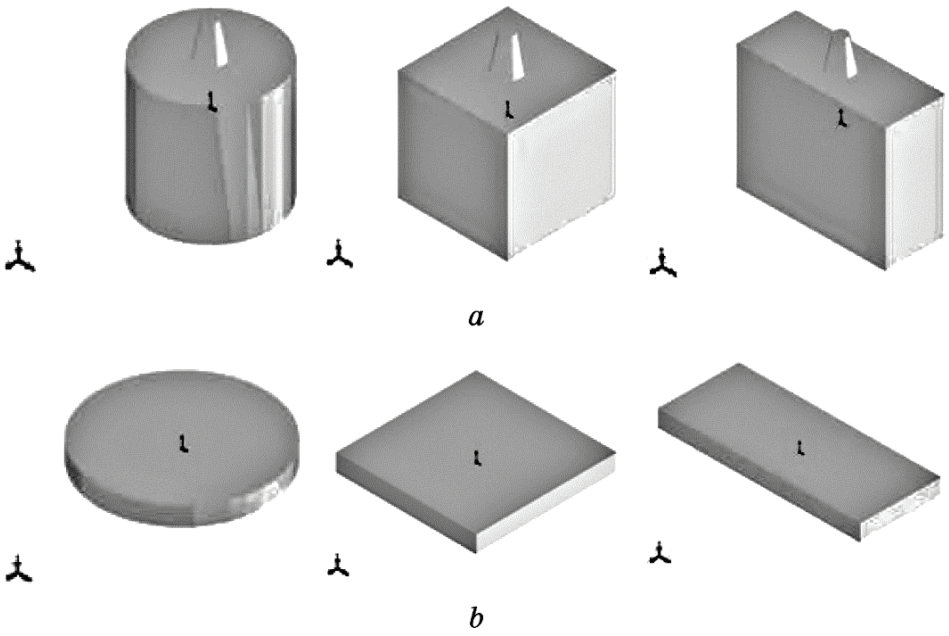

Fig. 1. Solid models for shrinkage studies: *a*—shrinkage, *b*—respective chills.

[15]. The solid models for shrinkage simulations were created using the SolidWorks software.

The solid models for shrinkage simulation are given in Fig. 1, along with their respective chills where applicable.

3.2. Simulation Studies

Casting process simulations were carried out using Virtual Casting software [15], which is a program for the simulation of the solidification process of industrial castings using FDM.

Virtual casting software creates a virtual environment for casting solidification, predicting and analysing the occurrence of shrinkage defects. The input data for the casting process simulation are solid model of the casting, material properties and boundary conditions.

Virtual Casting consists of three major processes: Pre-processing, Solving the governing equations and Post-processing or visualization of results. The simulation output/results were displayed as contour plots of temperature, porosity, solid fraction (Fs), solidification time and cooling rate.

For accurate results, the process simulation requires boundary conditions. The boundary condition values described at the beginning of the process were the thermal data of metal and casting mould, condi-

TABLE 5. Physical constants and properties of US A356, US 413 alloys, silica sand and mild steel chill for casting simulation.

Sl. No.	Parameter	US A356	US 413	Sand	MS Chill
1	Melting point, K	934	855	—	—
2	Thermal conductivity, W/(mm·K)	0.159249	0.121338	90.27×10^{-5}	4.5×10^{-2}
3	Density of solid, g/cm^3	2.68496	2.65772	1.5219	7.84
4	Liquids temperature, K	886	847	—	—
5	Freezing range, K	400	303.75	—	—
6	Latent heat of fusion, J/kg	388442	389112	—	—
7	Specific heat, J/(kg·K)	962.944	1170	1076.0076	460.548
8	Heat Transfer Coefficient, HTC, W/(m^2·K)				
	Metal–mould	35×10^{-4}	25×10^{-4}	—	—
	Metal–coating mould	15×10^{-4}	12×10^{-4}	—	—

tions of heat exchange between the casting and individual parts of the mould and between the mould and its surroundings.

The interfacial heat transfer coefficient is the rate of heat loss through the metal/mould interfaces, which influence the casting characteristics [16]. However, interfacial heat transfer coefficient is not a simple material property and is dependent upon chemical, physical interfacial conditions, mould and casting material properties and casting geometry. The selection of interfacial heat transfer coefficient values, as well as boundary conditions at the metal/mould interface, affects the accuracy of the simulations. In the present investigations, interfacial heat transfer coefficient values for conformity of computer simulation and the experimental measurements were consistent. The thermo-physical properties of US A356, US 413 alloys, silica sand and mild steel chill for the casting process simulation [16–18] are given in Table 5.

The solid model of shrinkage characteristic, which is imported in the STL-file format (Fig. 2) as the solution domain, divides into small finite cells of casting and mould with a material identification. Boundary conditions were assigned at all material interfaces metal, mould and mould coat.

The critical liquid fraction (a parameter used is the solvus in the governing equations for calculation of porosity) is the value of liquid fraction, below which a neighbouring cell does not feed to pay off for shrinkage. During solidification at a particular location, liquid is pulled in from neighbouring locations to pay off for solidification shrinkage. If the neighbouring location has a high percentage of solid, liquid cannot flow through it. The exit solid fraction is the total volume percent of solid, at which the simulation exits.

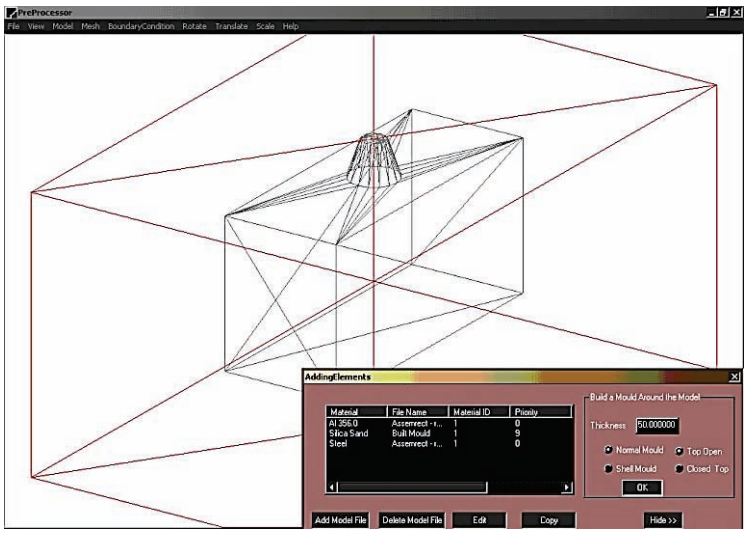

Fig. 2. STL-file and boundary conditions.

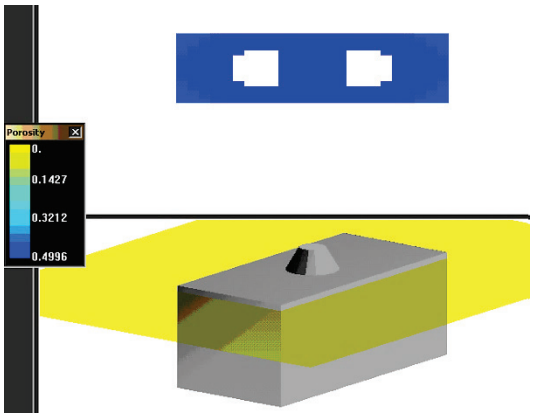

Fig. 3. Typical contour plots showing the porosity distribution for simulation 30.

For example, a value of 1 for the exit solid fraction means that the simulation will be done until the casting is 100% solidified. The simulation results for shrinkage are represented as contour plots of the location and magnitude of porosity formed during the solidification at particular location from the bottom of the casting for simulation run order 30 in Fig. 3.

In Figures 3 and 4, the top portion shows the magnitude of porosity formed during the solidification and the bottom portion depicts the location of the porosity from the bottom of the casting.

4. RESULTS AND DISCUSSION

The transformation from the liquid state to the solid state is accompanied by a decrease in volume in most metals, leading to shrinkage and porosity [1]. The tendency for the formation of shrinkage is associated with both liquid and solid volume fraction and the solidification temperature range of the particular alloy [1, 12]. Shrinkage occurs in metallic materials during freezing and cooling.

Using the virtual casting software, macroshrinkage and microshrinkage for the 36 simulation runs were done. The contour plots showing the location and magnitude of porosity formed during the solidification for simulation number 13 is shown in Fig. 4, in 2D, which is difficult to measure. Hence, 3D solid works software was used for generating 3D model of the images. The large tolerance level (0.1 mm), typical in foundry processes [19] was considered for the present study. Post processing image is converted to the solid model part (SLD-part) file format. The starting location of the shrinkage porosity was 80 mm from bottom and spread up to 92 mm from the flat bottom. These con-

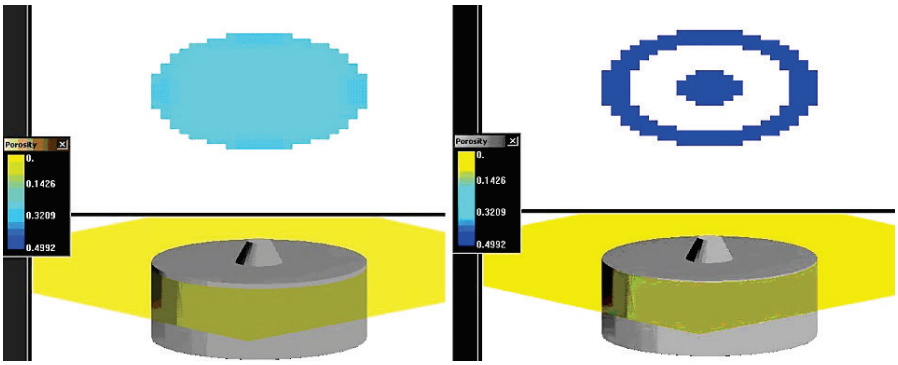

Fig. 4. Typical contour plots showing the porosity distribution for simulation 13.

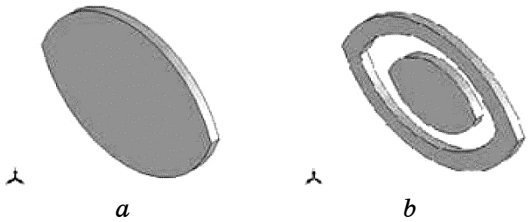

Fig. 5. Constructed porosity of the simulation run order 13: *a*—84 mm from bottom (volume is 15.49288 cm^3), *b*—88 mm from bottom (volume is 10.8578 cm^3).

TABLE 6. Shrinkage porosity distribution—Simulation 13.

Sl. No.	Distance from the flat bottom, mm	Volume, cm^3
1	80	15.49288
2	84	10.63793
3	88	10.85780
4	92	15.55000
	Total volume	52.53861

TABLE 7. Amount of Shrinkage porosity—Simulation 13.

Total volume of shrinkage porosity distribution, cm^3	52.53861
Amount of shrinkage porosity distribution in the four regions, cm^3	$52.53861 \times 0.499 = 26.21677$
Amount of shrinkage porosity in the casting, cm^3	$26.21677/572.265 = 0.045812$
Percentage shrinkage porosity in the casting	4.5812

tour plot data were converted to solid model part (SLD-part) was shown as constructed porosity in Fig. 5 (for 84 mm and 88 mm).

The shrinkage porosity distribution for simulation 13 between 80–92 mm from the flat bottom was given in Table 6. The porosity distribution obtained from the contour plot in all the four locations was 0.499. The amount of shrinkage porosity distribution in these regions is given in Table 7.

The porosity distribution for all the 36 simulations was calculated in similar way. Figure 6 gives the constructed porosity of simulation for run 5 and 30 for rectangle (103 mm from bottom, volume is 10.399 cm^3 and 108 mm from bottom, volume is 9.4899 cm^3) and cube (68 mm from bottom, volume is 6.02598 cm^3 and 72 mm from bottom, volume is 6.20088 cm^3) castings respectively.

The porosity distribution results for all the 36 simulations are given in Table 8.

4.1. Solidification

When liquid metal enters a mould cavity, its heat is absorbed and transferred through the mould wall as shown in Fig. 7. For eutectics and pure metals, the solidification continues layer by layer starting from the mould wall and gradually moving inwards [21]. The progressing layer between the liquid and solid is called the solidification front.

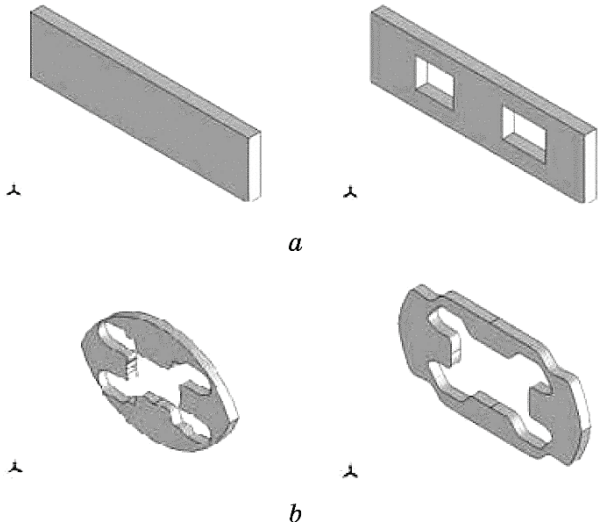

Fig. 6. Shows constructed porosity of simulation for run: *a*—30, rectangle casting; *b*—5, cube casting.

As this front solidifies, it contracts in volume, and draws liquid metal from the inner part of the casting (opposite to the mould wall).

When the solidification front reaches the innermost region or the thickest part of the casting, there is no liquid metal left to compensate the shrinkage, and as a result, a void space called shrinkage cavity is formed.

When liquid metal enters into the mould cavity, its heat is removed and transferred through the mould wall. Most of the cast alloys do not have distinct melting point. Only pure metals and eutectic alloys solidify at a constant temperature. However, cast alloys solidify over a

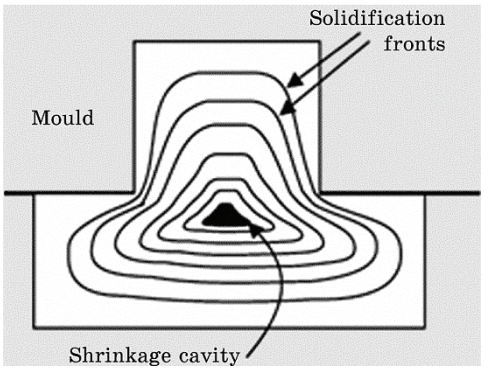

Fig. 7. Solidification of casting in a mould.

TABLE 8. Porosity distribution for all 36 simulations.

Simulation run order	Alloy	Chill	Pouring temperature, °C	Mould coat	Casting mould	Shrinkage porosity, %
1	US A356	MS	$T + 50$	GC	Cylinder	3.473
2	US A356	MS	$T + 50$	GC	Cube	2.845
3	US A356	MS	$T + 50$	GC	Rectangle	2.628
4	US A356	MS	$T + 50$	NC	Cylinder	3.500
5	US A356	MS	$T + 50$	NC	Cube	3.162
6	US A356	MS	$T + 50$	NC	Rectangle	2.700
7	US A356	MS	T	GC	Cylinder	3.850
8	US A356	MS	T	GC	Cube	3.250
9	US A356	MS	T	NC	Rectangle	2.800
10	US A356	No	$T + 50$	NC	Cylinder	3.800
11	US A356	No	$T + 50$	NC	Cube	3.240
12	US A356	No	$T + 50$	GC	Rectangle	2.895
13	US A356	No	T	GC	Cylinder	4.582
14	US A356	No	T	GC	Cube	3.300
15	US A356	No	T	GC	Rectangle	3.100
16	US A356	No	T	NC	Cylinder	4.515
17	US A356	No	T	NC	Cube	3.500
18	US A356	No	T	NC	Rectangle	3.130
19	US 413	MS	T	NC	Cylinder	3.380
20	US 413	MS	T	NC	Cube	2.900
21	US 413	MS	T	NC	Rectangle	2.180
22	US 413	MS	T	GC	Cylinder	3.340
23	US 413	MS	T	GC	Cube	2.880
24	US 413	MS	T	GC	Rectangle	2.190
25	US 413	MS	$T + 50$	NC	Cylinder	3.040
26	US 413	MS	$T + 50$	NC	Cube	2.610
27	US 413	MS	$T + 50$	NC	Rectangle	2.000
28	US 413	No	T	GC	Cylinder	3.400
29	US 413	No	T	GC	Cube	2.710
30	US 413	No	T	GC	Rectangle	2.290
31	US 413	No	$T + 50$	NC	Cylinder	3.350
32	US 413	No	$T + 50$	NC	Cube	2.640
33	US 413	No	$T + 50$	NC	Rectangle	2.100
34	US 413	No	$T + 50$	GC	Cylinder	3.300
35	US 413	No	$T + 50$	GC	Cube	2.600
36	US 413	No	$T + 50$	GC	Rectangle	2.120

range of temperatures. The range between the liquidus line and solidus line is known as the freezing range $R_f = T_{liq} - T_{sol}$, where T_{liq} is liquidus temperature and T_{sol} is solidus temperature as shown in Fig. 8.

Solidification proceeds layer-by-layer in short freezing range (US 413) alloys, which behave like pure metals and eutectics. Solidification is initiated at a large number of nucleation sites, in case of long

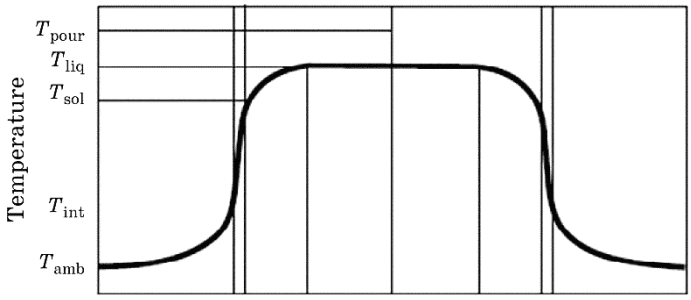

Fig. 8. Freezing range of alloys.

freezing range alloys and grains grows until the neighbouring grains hinder them. Freezing rate is greatly affected by the cooling rate and thermal gradients inside the casting, which are influenced by varying process parameters.

4.2. Influence of Process Parameters

4.2.1. Casting Mould

Progress of solidification is influenced by size, shape and thickness of the casting [18, 20]. Macrocavities decrease with casting shape changes from thick cylinder to thin rectangle castings. The shape of the casting influences the solidification of the casting in localized areas because the edges play a significant role in the heat extraction. The edges of the test casting, combined with the relative composition of the alloy, decide the variation in formation of macrocavities. The solidification time is inversely proportional to surface area of the casting [22].

Relative solidification time affects the macrocavities (with increased solidification time, the macrocavities increase). Solidification time is higher in cylindrical shape castings (which have the least surface area of the three casting shapes considered for the present study) [22], which promoted maximum macrocavities. The influence of casting shape on shrinkage porosity is shown for the two alloys US A356 and US 413 in Figs. 9 and 10. The numbers 1–6 on the X-axis in the Figs. 9 and 10 were percentage shrinkage values obtained for six simulation runs conducted for each casting mould.

4.2.2. Chill

Bottom chills reduced the shrinkage porosity for all the shapes of castings (rectangle, cube and cylinder). Bottom chill extracts heat locally. However, there was an increased rate of heat extraction from the liq-

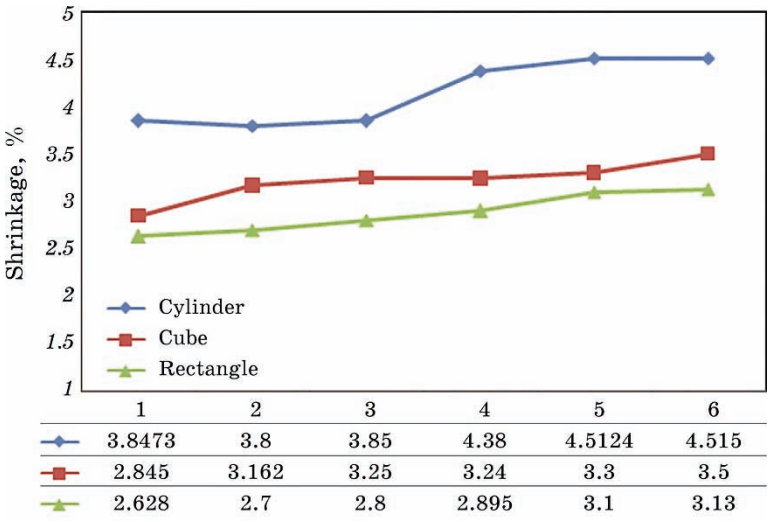

	1	2	3	4	5	6
Cylinder	3.8473	3.8	3.85	4.38	4.5124	4.515
Cube	2.845	3.162	3.25	3.24	3.3	3.5
Rectangle	2.628	2.7	2.8	2.895	3.1	3.13

Fig. 9. Influence of casting mould on shrinkage—US A356.

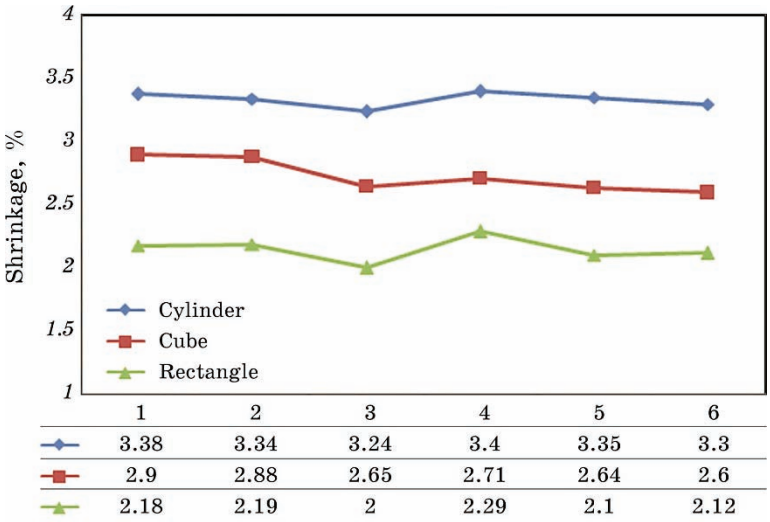

	1	2	3	4	5	6
Cylinder	3.38	3.34	3.24	3.4	3.35	3.3
Cube	2.9	2.88	2.65	2.71	2.64	2.6
Rectangle	2.18	2.19	2	2.29	2.1	2.12

Fig. 10. Influence of casting mould on shrinkage—US 413.

uid metal and compensation of solidification shrinkage as the pouring time of molten metal increased, giving a reduction in shrinkage porosity.

The rate of heat extraction and the temperature gradients inside the solidifying metal influenced the solidification. Changes in temperature gradient by the presence of chill had no effect on macrosolidifica-

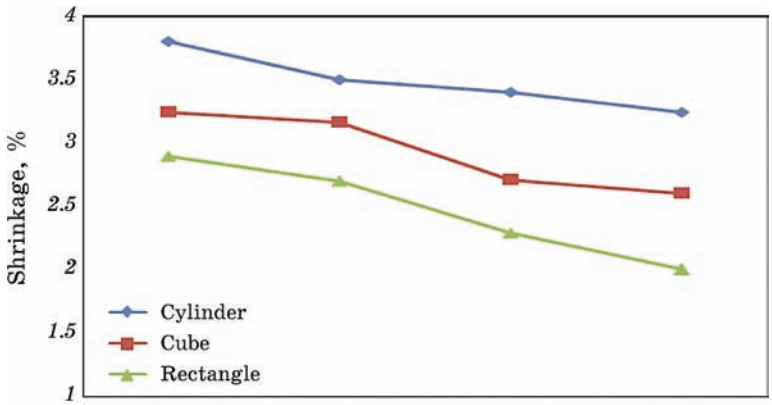

	US A356 No Chill	US A356 Chill	US 413 No Chill	US 413 Chill
Cylinder	3.8	3.5	3.4	3.24
Cube	3.24	3.16	2.71	2.6
Rectangle	2.895	2.7	2.29	2

Fig. 11. Influence of chill on shrinkage.

tion and hence macrocavities were not influenced. Chills promoted steeper temperature gradients in the solidifying metal and increased the feeding capacity, thus reducing internal porosity and pore size. The influence of a bottom chill on the shrinkage porosity is given in Fig. 11.

4.2.3. Pouring Temperature

Pouring temperature is an important parameter in foundries for manufacturing quality castings. In order to study the influence of pouring temperature on shrinkage porosity, pouring temperature, T, and $T + 50$°C were considered. Superheat is the additional heat essential for melting, which increases the fluidity and provides the allowance for heat losses before they are in their final position in the mould. Increased pouring temperature results in lower rate of heat extraction by the mould, hence higher pouring temperature led to decreased macrocavities and internal porosity as shown in Fig. 12.

4.2.4. Mould Coat

In order to study the effect of mould coating on shrinkage porosity, moulds with and without graphite coatings were considered. Mould coatings provide smooth casting surfaces and influence the thermal gradient by promoting the directional solidification. Mould coatings

allow a passageway for feed metal to flow into the solidifying structure and compensated for normal metal shrinkage during solidification. There was decreased shrinkage porosity for all the three types of casting shapes in graphite-coated moulds as shown in Fig. 13.

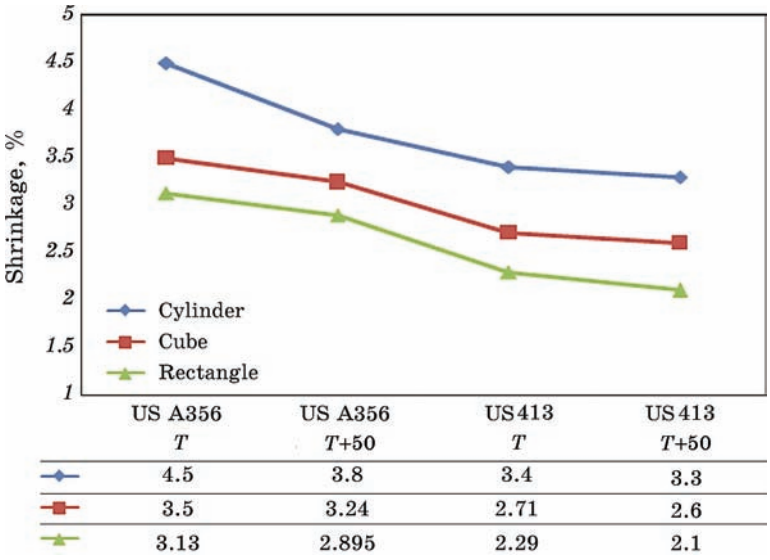

	US A356 *T*	US A356 *T*+50	US413 *T*	US413 *T*+50
Cylinder	4.5	3.8	3.4	3.3
Cube	3.5	3.24	2.71	2.6
Rectangle	3.13	2.895	2.29	2.1

Fig. 12. Influence of pouring temperature on shrinkage.

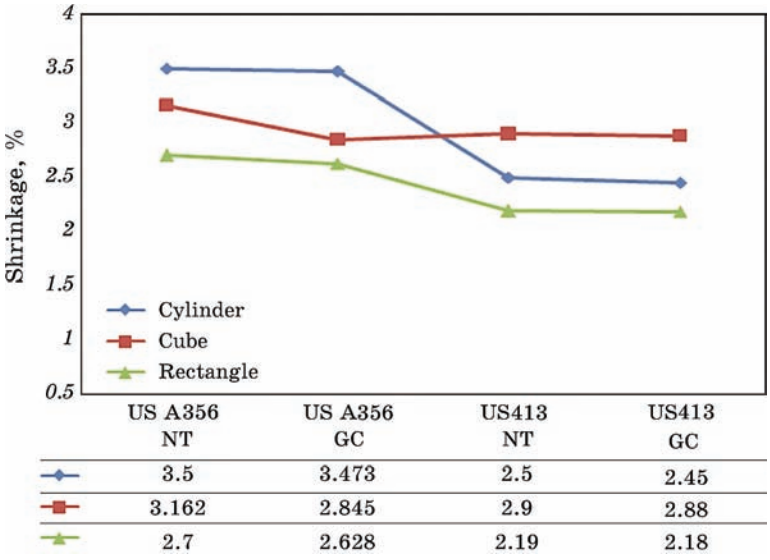

	US A356 NT	US A356 GC	US413 NT	US413 GC
Cylinder	3.5	3.473	2.5	2.45
Cube	3.162	2.845	2.9	2.88
Rectangle	2.7	2.628	2.19	2.18

Fig. 13. Influence of mould coat on shrinkage.

4.2.5. Interaction Plots

The importance of interactions among influencing factors are illustrated using interaction plots. The effect of one factor is dependent upon the other. To study interaction effects between the process parameters, it is necessary to vary all the factors simultaneously. If the process parameters are more than three, then, the interaction plot can be displayed in the form of matrix. The plot has one panel for each pair of factors in the data set.

Parallel lines in the interaction plot imply no interaction between the influencing factors. Increased departure from parallel plots implies stronger interaction effects.

A significant amount of interaction was observed between the processing parameters. The interaction and main effects plot (given in Figs. 14 and 15) for shrinkage indicate that there was a strong interaction among all the influencing factors, when considering the levels (variables). Thus, the alloy, bottom chill, mould coat, casting shape

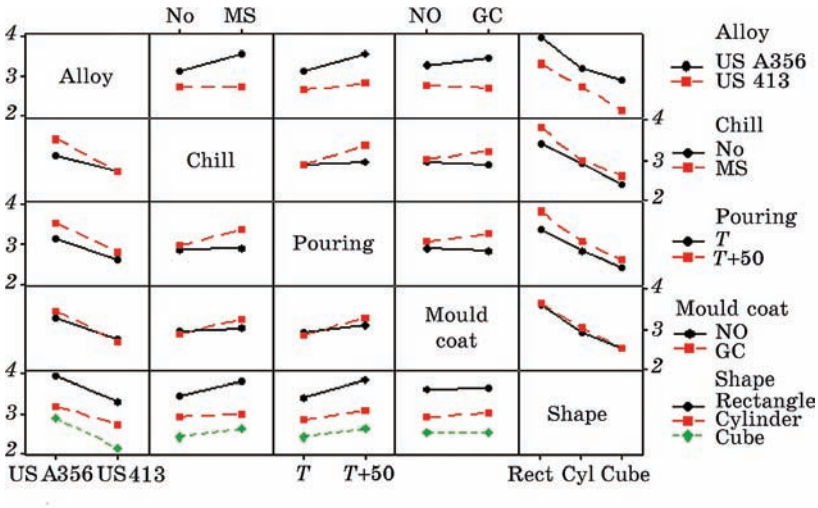

Fig. 14. Interaction plots of processing parameters on shrinkage.

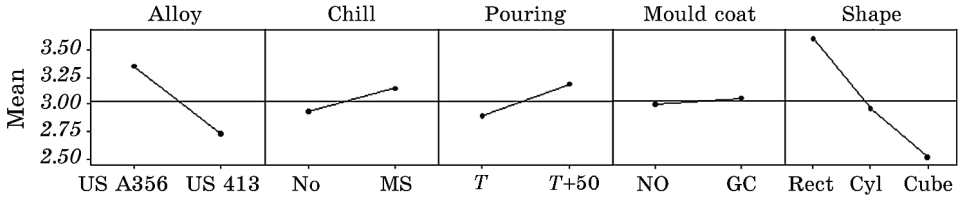

Fig. 15. Plots showing the processing parameters on shrinkage.

and pouring temperature influence the shrinkage. The difference in the vertical position of the plotted points indicates greater magnitude of the effect, hence the bottom chill factor is considered more significant in influencing shrinkage.

5. EXPERIMENTAL VALIDATION STUDIES

Experiments were conducted to validate the casting process simulation results. To evaluate the influence of process parameters, six experiments were conducted (given in Table 9), and a schematic diagram of the testing arrangement for cube casting is shown in Fig. 16. These experiments were designated as experiments run order 1 to 6. The prepared moulds, overflow core and pouring basins for three casting shapes are shown in Fig. 17. The overflow core was placed over the mould in order to ensure that only a fixed quantity of metal was poured into the mould each time.

5.1. Moulding, Melting and Pouring

Moulds were prepared using green sand process. The sand composition

TABLE 9. Conditions for validation experiments.

Experiment run order	Alloy	Chill	Pouring temperature, °C	Mould coat	Casting shape
1	US A356	MS	$T + 50$	NC	Cylinder
2	US A356	MS	$T + 50$	GC	Cube
3	US A356	MS	T	NC	Rectangle
4	US 413	MS	T	NC	Rectangle
5	US 413	No	$T + 50$	GC	Cube
6	US 413	MS	T	NC	Rectangle

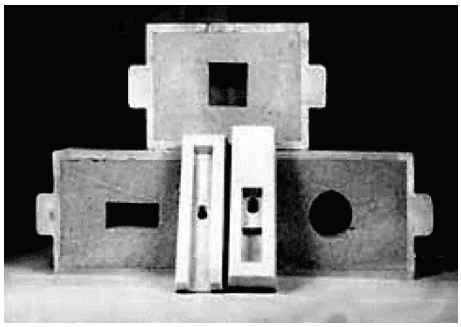

Fig. 16. The assembled mould for volume deficit experiment.

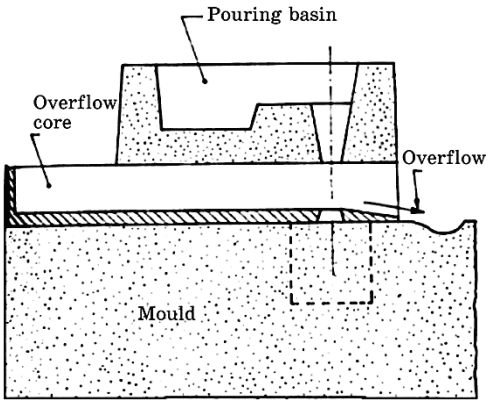

Fig. 17. Schematic diagram for the volume deficit experiment for cube shape casting.

was silica sand with 5–6 wt.% Bentonite and 5–8 wt.% water. Moulds were prepared with slight ramming. The patterns stripped after 3 hours. The alloy was melted in an electric resistance furnace of capacity 20 kg provided with mild steel crucible. Temperature was measured with a K-type thermocouple.

The furnace was turned off and the crucible was lifted and put in a tilting device. The metal was tapped into a smaller crucible for pouring into the mould. Figure 18 shows the solidified castings of the validation experiments.

Low-magnification examination of cast components reveals porosity, shrinkage. Unetched condition generally discloses the porosity and shrinkage defects. During solidification of casting, if a region in the casting receives insufficient amount of liquid metal, then, the liquid in this region solidifies either in the form of shrinkage/pore. Structure consists of a network of silicon particles (sharp and grey), formed in the interdendritic aluminium-silicon eutectic, for alloy US A356, as sand cast is shown in Fig. 19, while the structure consists of eutectic

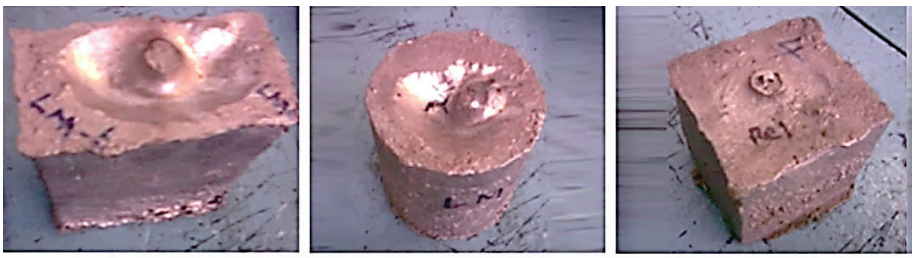

Fig. 18. Solidified castings from the validation experiments.

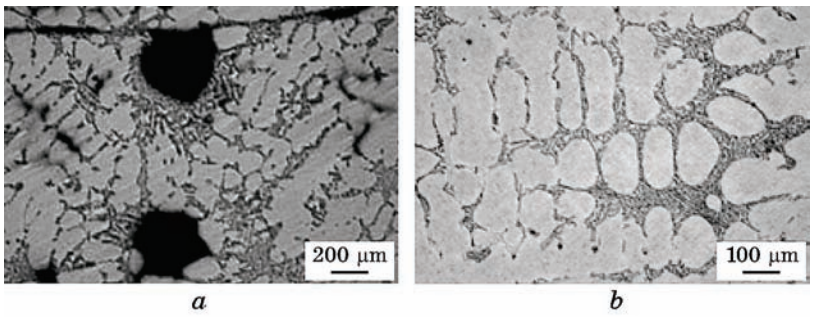

Fig. 19. Alloy US A356, as sand cast.

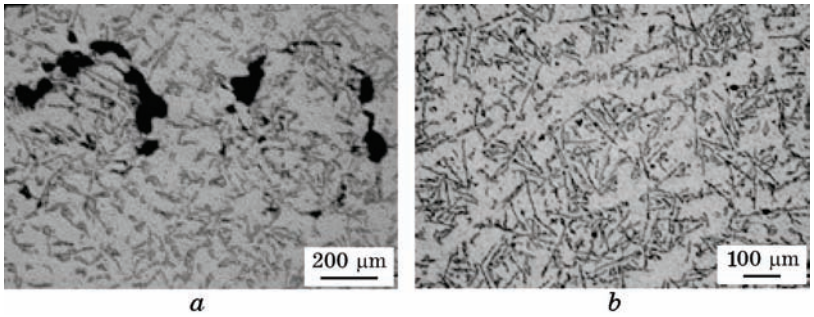

Fig. 20. Alloy US 413, as sand cast.

silicon (grey constituent) for alloy US 413, as sand cast is shown in Fig. 20 at 50× magnification.

5.2. Shrinkage Porosity Calculations for the Validation Experiments

Shrinkage porosity calculations for the validation experiments were done using Archimedes principle. The shrinkage porosity values for the six validation experiments are given at Table 10.

5.3. Comparison of Simulation and Experimental Studies

To establish the strength of association between the casting process simulation and experimental validation studies, correlation co-efficient between the two results is calculated using the formula:

$$\text{correlation}(r) = \frac{N\sum XY - \sum X \sum Y}{\sqrt{\left[N\sum X^2 - \left(\sum X\right)^2\right]\left[N\sum Y^2 - \left(\sum Y\right)^2\right]}},$$

TABLE 10. Shrinkage porosity values for the six validation experiments.

Experiment run order	Alloy	Chill	Pouring temperature, °C	Mould coat	Casting mould	Shrinkage porosity, %
1	US A356	MS	$T + 50$	NC	Cylinder	2.84
2	US A356	MS	$T + 50$	GC	Cube	2.65
3	US A356	MS	T	NC	Rectangle	2.63
4	US 413	MS	T	NC	Rectangle	2.11
5	US 413	No	$T + 50$	GC	Cube	2.07
6	US 413	MS	T	NC	Rectangle	1.90

where N is number of values (casting shape), X is shrinkage value of casting process simulation, Y is shrinkage value of experimental validation study.

The correlation coefficient value obtained was 0.9389 indicating a strong, positive relationship between casting process simulation and validation experiments for US 413 alloy as shown in Fig. 21.

The value of correlation coefficient for US A356 alloy was calculated similarly and is equal to 0.9353, indicating a strong association between the two studies.

The simulation results are in agreement with validation experiments data.

The casting process simulation results are in agreement with validation experiments, however minor variation is observed. During solidification, the mould cavity continuously changes the properties of liq-

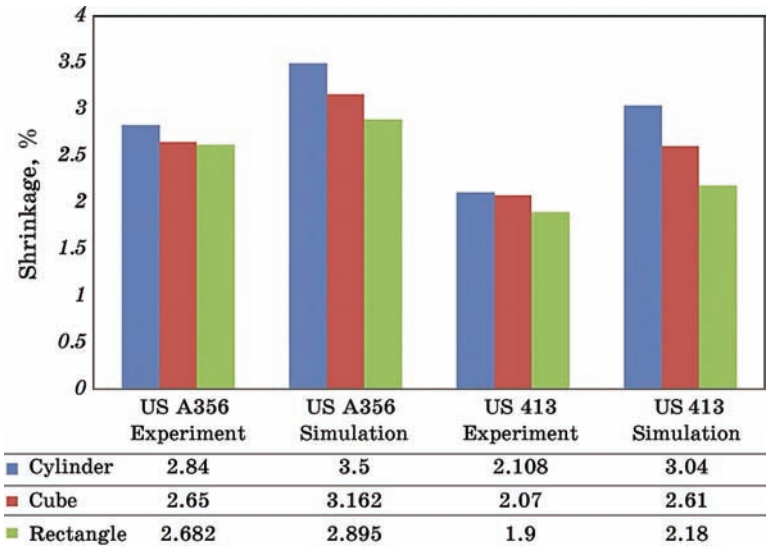

Fig. 21. Shrinkage porosity: simulation and experimental studies.

uid and solid phases due to interactions between metal-mould, metal-ambient and mould-ambient. Exactly envisaging the change in properties during solidification is very difficult in virtual environment (casting simulations). Interfacial heat transfer coefficient (h) is one of the critical properties of casting process simulation. Although mould and interface are considered as one and the same, certain mechanisms occur and change the h value during the casting process. It is necessary to obtain precise experimental data for mould coat, to study the effect of heat transfer coefficient accurately. Due to the above factors, there could be minor variation between the study results of casting process simulation and validation experiments.

6. CONCLUSION

For casting process simulation and experimental validation studies, the correlation coefficient value obtained is observed to be close to +1 indicating a positive relationship between them. The thermal insulation properties of the mould coating played a vital role in shrinkage of the casting. The mould coating was designed to absorb the gaseous products formed at the metal front thereby reducing the shrinkage. Shrinkage decreased with changed casting shape, from cylinder to rectangle castings. Higher pouring temperature resulted in lower rates of heat extraction by the mould, thereby decreasing macro- and microshrinkage. Chill promoted faster temperature gradient in the solidifying metal and increase its feeding capacity thereby reducing shrinkage.

ACKNOWLEDGEMENTS

The authors thank the Directorate of Engineering and the Director, DRDL for providing support and permission for carrying out this R&D work.

REFERENCES

1. *ASM Metals Handbook. Vol. 15. Casting* (Eds. S. Viswanathan, D. Apelian, R. DasGupta, M. Gywn, J. L. Jorstad, R. W. Monroe, T. E. Prucha, M. Sahoo, E. S. Szekeres, and D. Twarog) (ASM International: 2008).
2. *Foundry Rejects Old Conventional Approach of Trial and Error and Adopts Computer Simulation* (Eds. A. Sholapurwalla, S. Scott, and C.-A. Rolle) (Casting Engineer: 2010).
3. Durgesh Joshi and B. Ravi, *Indian Foundry J.*, **56**, No. 1: 23 (2010).
4. S. Venkateswaran, R. M. Mallya, and M. R. Seshadri, *AFS Trans.*, **94**: 67 (1986).
5. *Experiment Design & Analysis Reference* (Tucson, Arizona, USA: 2008).

6. *Design of Experiments Guide. JMP, A Business Unit of SAS, SAS Campus Drive, Cary, NC 27513* (2010).
7. *Minitab 16. User Manual of MINITAB* (2008).
8. D. Hanumantha Rao, G. R. N. Tagore, and G. Rangajanardhan, *Indian Foundry J.*, **52**, No. 5: 26 (2006).
9. S. Sundarrajan, H. Md. Roshan, and E. G. Ramachandran, *Trans. Indian Institute of Metals*, **37**, No. 4: (1984).
10. S. Sundarrajan, H. Md. Roshan, and E. G. Ramachandran, *Proc. 37th ATM of IIM (Varanasi, India, 1983)*, p. 119.
11. S. Sundarrajan, H. Md. Roshan, and E. G. Ramachandran, *Proc. IIF, 32nd Annual Conference (1983)*, p. 21.
12. *Foseco Non-Ferrous Foundryman's Handbook. Eleventh Edition* (Ed. J. R. Brown) (Butterworth Heinemann Publisher: 1999).
13. *User Manual Virtual Casting Developed by Regional Research Laboratory* (Trivandrum, India: 2006).
14. M. Trovant, *A Boundary Condition Coupling Strategy for the Modeling of Metal Casting Processes* (Disser. for PhD) (Toronto, Canada: Graduate Department of Metallurgy and Materials Science University of Toronto: 1998).
15. M. Venkataramana, V. Vasudeva Rao, R. Ramgopal Varma, and S. Sundarrajan, *J. Instrum. Soc. India*, **37**, No. 3: 157 (2008).
16. G. S. Cellini and L. Tomesani, *J. Achiev. Mater. Manuf. Eng.*, **29**, Iss. 1: 47 (2008).
17 J. Campbell and R. A. Harding, *The Fluidity of Molten Metals (TALAT Lecture 3205)* (The University of Birmingham, United Kingdom: 1994).
18. P. C. Mukherjee, *Fundamentals of Metal Casting Technology* (India: Oxford & IBH Pub. Co.: 1988).
19. J. Nukaga, S. Kitazawa, and H. Kamimura, *NDT & E International*, **41**, Iss. 7: 564 (2008).
20. L. Arnberg, *Solidification Characteristics of Aluminium Alloys, Dendrite Coherency* (AFS: 1996), vol. **3**.
21. R. F. Mehl, *Proc. of Symp. 'The Solidification of Metals and Alloys' (Feb. 12, 1951)* (New York, USA: AIME: 1951), p. 24.
22. R. W. Heine, C. R. Loper Jr., and P. C. Rosenthal, *Principles of Metal Casting* (New York, USA: McGraw-Hill: 1967).